JACS Au
AN OPEN ACCESS JOURNAL OF THE AMERICAN CHEMICAL SOCIETY

pubs.acs.org/jacsau
Article

Light-Sensitive Ion Channel Delivery System for Ion-Interference Tumor Therapy

Yueyue Lu, Yuxin Wu, Canhong Zhu, Tianlong Zhang, Yanting Wu, Lulu Xi, Xianze Huang, Tengfei Yan,* and Junqiu Liu*

Cite This: JACS Au 2025, 5, 4439−4448
Read Online
ACCESS | Metrics & More | Article Recommendations | Supporting Information

ABSTRACT: Artificial ion channels have shown great potential applications in tumor treatment by disrupting ion homeostasis across cancer cell membranes. Herein, we report a de novo-designed ion channel delivery system (ICDS) based on light-sensitive nanocapsules that can induce cell apoptosis via interfering with ion homeostasis of subcellular membranes of tumors. The nanocapsules were self-assembled by the host−guest complex of azobenzene-modified quinoline helix (an artificial proton channel) and α-cyclodextrin, which can easily enter tumor cells by an endocytic effect and release proton channels under ultraviolet (UV) light irradiation. The artificial proton channels further neutralize the acidic organelles (such as lysosomes), deplete the mitochondrial membrane potential, elevate reactive oxygen species (ROS) levels, and eventually induce the apoptosis of cancer cells. As far as we know, this is the first example of an ion-interference antitumor strategy by an ion channel delivery system that may offer novel therapeutic directions for artificial ion channels.

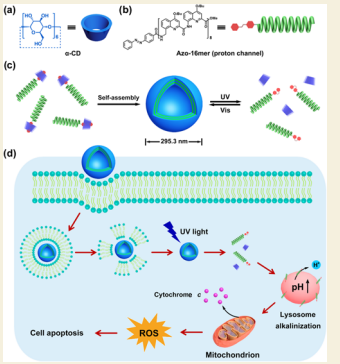

KEYWORDS: *quinoline helix, nanocapsule, artificial proton channel, ion channel delivery system, cell apoptosis*

INTRODUCTION

In living systems, transmembrane ion channel proteins play essential roles in a wide range of physiological functions, such as regulating osmotic pressure, neural signal transmission, muscle contraction, and relaxation.[1] Dysfunctions of ion channel proteins may cause a variety of life-threatening diseases, such as hypertension, endocrine disorders, cystic fibrosis, etc.[2] Recent studies revealed that the synthetic ion channels can not only help to understand the working mechanism of their natural counterpart but also serve as potential candidates for alleviating the discomfort of channelopathies.[3−5] For example, in 2019, Burke and co-workers demonstrated that a small cyclic molecule, amphotericin B, can insert into the cell membranes and form transmembrane anion channels, restoring the physiological functions of the cystic fibrosis transmembrane conductance regulator (CFTR) in epithelial cells.[6] Another life-threatening disease, liver fibrosis, is also closely related to the dysregulation of intracellular K^+ homeostasis.[7] In 2024, Ren and co-workers demonstrated that the artificial K^+-selective transporter is capable of reversing liver fibrosis according to both in vitro and in vivo experiments.[8] In addition, the synthetic cation/anion channels can also interfere with the ion homeostasis of tumor cells and further trigger programmed death of cancerous cells.[9] For example, Talukdar and co-workers have realized cancer cell apoptosis by using supramolecular artificial Cl^- channels to disrupt the cellular ionic homeostasis, which further facilitated the deacidification of lysosomes or even disrupted autophagy in cancer cells.[10−12] Very recently, Ren and co-workers reported a ROS-responsive artificial H^+/Cl^- channel, which can be activated by the elevated ROS levels in cancer cells. The synergistic transport of H^+ and Cl^- could induce significant apoptotic activity against human breast cancer cells.[13] The rapid development of nanochannel-based anticancer treatment provides a new therapeutic strategy through destruction of the ion gradients across the plasma membranes of cancer cells, which is reminiscent of the well-known ion-interference therapy (IIT). In 2019, Bu and co-workers utilized the pH-sensitive CaO_2 nanoparticles to induce "calcium overload" under the tumor microenvironment, leading to metabolic/proliferative dysfunction and cell death with calcification.[14] The core principle of IIT is disrupting the ion homeostasis to inhibit the proliferation of cancerous cells.[15] Similarly, artificial ion channels can also trigger cancer cell apoptosis by disrupting the Na^+, K^+, or Cl^- homeostasis across cellular membranes, which therefore can be regarded as a supplementary to the IIT.[16−19]

As is known, the channel proteins not only play pivotal roles on the plasma membrane but also facilitate unique physiological functions in organelle membranes.[20,21] In recent

Received: June 25, 2025
Revised: August 15, 2025
Accepted: August 19, 2025
Published: August 23, 2025

https://doi.org/10.1021/jacsau.5c00762
JACS Au 2025, 5, 4439−4448

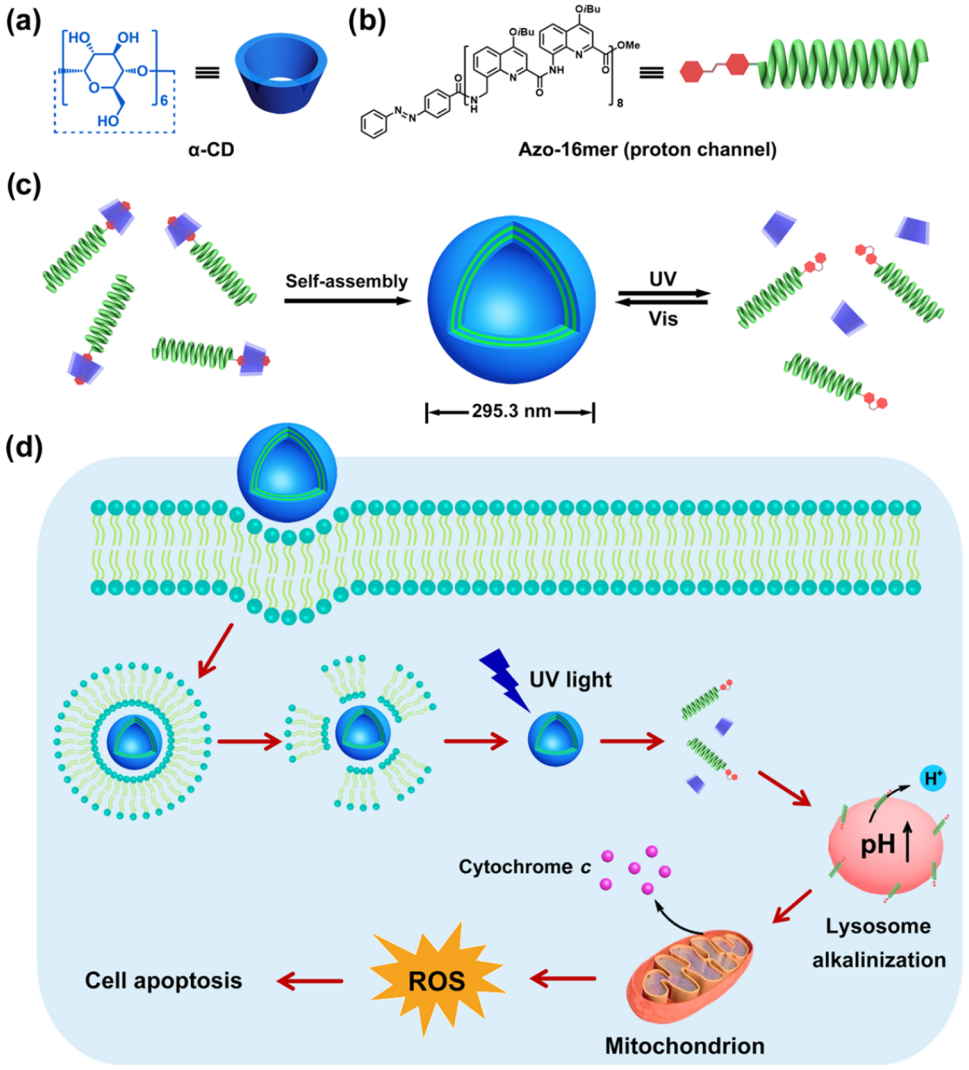

Figure 1. Chemical structures and cartoon illustrations of (a) α-CD and (b) **Azo-16mer**. (c) The schematic representation of supra-amphiphilic helix-based nanocapsules with reversible light-sensitive disassembly−reassembly behaviors. (d) Cartoon illustration of the cell apoptosis process induced by supra-amphiphilic helix-based nanocapsules through the ion channel delivery system.

years, chemical researchers have tried to disrupt the ion homeostasis of subcellular membranes to enhance the efficacy of ion-interference anticancer therapy. For example, in 2020, Yang and co-workers reported a synthetic K^+ transporter that can selectively mediate K^+/H^+ transport on the mitochondrial and lysosomal membranes, revealing cytotoxicity to chemo-resistant ovarian cancer stem cells (CSCs) via apoptosis induction and autophagy suppression.[22] In 2024, Gale and co-workers reported subcellular-targeted anionophores by introducing organelle-specific motifs to a naphthalimide scaffold with anion binding and transmembrane transport abilities, which have shown enhanced cytotoxicity toward cancerous cell lines.[23] Even though some efforts have been devoted to this field, the investigation of artificial ion transport behaviors within organelle membranes is still not easy due to the complicated preparation and characterization procedures. As is known, the traditional drug delivery system (DDS) is always applied for the controlled release of anticancer agents with enhancing and targeting abilities.[24,25] Therefore, we wondered whether we can deliver artificial ion channels into cells by developing a similar delivery system.

We herein report a light-sensitive supramolecular nanocapsule based on artificial ion channels that can be delivered into the cytosol of tumor cells through endocytosis, further disrupting the ion homeostasis and inducing cancer cell apoptosis. Therefore, we named it the ion channel delivery system (ICDS) inspired by the IIT and DDS. Briefly, the nanocapsules were self-assembled by the host−guest complex of hydrophilic α-cyclodextrin (α-CD) and a hydrophobic azobenzene-modified helix (an artificial proton channel), which could release artificial proton channels inside tumor cells under UV light irradiation. The helix-based proton channels will further neutralize lysosomal pH, deplete the mitochondrial membrane potential (MMP), increase reactive oxygen species (ROS) levels, and eventually induce significant apoptosis of cancer cells (Figure 1). To the best of our knowledge, such a light-responsive ion-interference tumor therapy by an ion channel delivery mechanism has never been reported so far.

https://doi.org/10.1021/jacsau.5c00762
JACS Au 2025, 5, 4439−4448

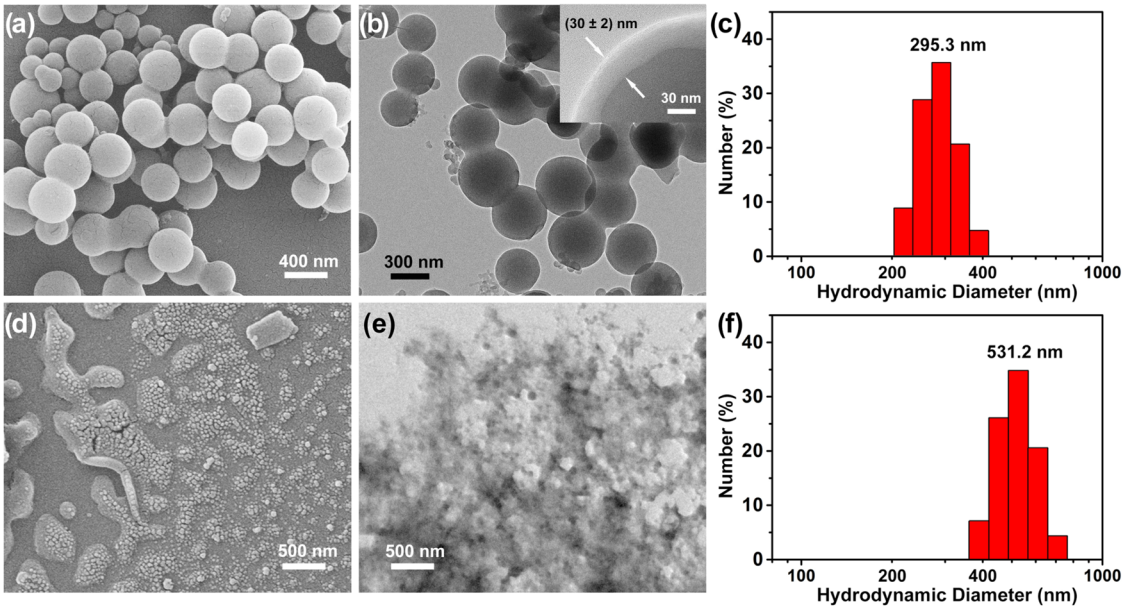

Figure 2. (a) SEM, (b) TEM, and (c) DLS measurements of the supramolecular nanocapsules self-assembled by the supra-amphiphilic helix (**Azo-16mer** ⊂ α-CD) at a concentration of 10^{-5} M in aqueous solution. (d) SEM, (e) TEM, and (f) DLS measurements of the supramolecular nanocapsules after irradiating with the UV light (365 nm, 3 W) for 10 min.

RESULTS AND DISCUSSION

Molecular Design and Morphological Characterization

In order to construct the light-sensitive ICDS, α-CD and azobenzene-containing aromatic foldamer Azo-$(mQQ)_8$-Me (denoted as **Azo-16mer**, Q: 8-amino-2-quinoline carboxylic acid; mQ: 8-aminomethyl-2-quinoline carboxylic acid) were selected as host and guest molecules, respectively (Figure 1a,b and Scheme S1), which could form a supra-amphiphilic helix (**Azo-16mer** ⊂ α-CD) and further self-assemble into supramolecular nanocapsules at a concentration of 0.05 mM in aqueous solution. According to our previous reports,[26] this kind of supra-amphiphilic helix-derived nanocapsules qualified with reversible disassembly−reassembly performances under alternate UV/vis light irradiation. Because the α-CD prefers to recognize the *trans*-isomer but excludes the bulky *cis*-isomer of azobenzene groups due to the mismatched spatial conformation (Figure 1c).[27] In 2021, we also found that this quinoline helix can form a transmembrane channel with high proton selectivity. Because the quinoline helix-based channel possesses a small luminal cavity of 1 Å in diameter, which could efficiently reject the permeation of cations, anions, or water molecules but only permits the translocation of protons owing to the size effect.[28] Therefore, we introduced a light-sensitive azobenzene group into this artificial helix and acquired **Azo-16mer** with the same proton transport abilities.

The morphological structures of the supra-amphiphilic helix-based nanocapsules were first characterized by scanning electron microscopy (SEM) and transmission electron microscopy (TEM) instruments. As shown in Figure 2a,b, the self-assembled nanocapsules exhibited well-defined hollow spheres and the membrane thickness of nanocapsules was clearly visualized to be about (30 ± 2) nm according to the high-resolution TEM (the inset of Figure 2b), indicating a multiple-layer membrane structure based on the theoretically simulated length of the host−guest complex of **Azo-16mer** ⊂ α-CD (Figure S1). Additionally, dynamic light scattering (DLS) measurements were further performed and showed that the overall diameter of the nanocapsules was about 295.3 nm in aqueous solution (Figure 2c). As is well-known, the *trans*-azobenzene group can be easily recognized by the hydrophobic cavity of α-CD. After being irradiated by UV light, the *trans*-azobenzene will transform into its *cis*-isomer with a bigger size and then be extruded out from α-CD owing to the mismatched spatial conformation.[27] It is conceivable that the disassembly process of supramolecular nanocapsules could be easily achieved using UV light as the driving force.

Therefore, the UV−vis spectroscopy was first employed to examine the photoisomerizing abilities of **Azo-16mer**; it was worth noting that two characteristic absorption bands at 325 and 440 nm have, respectively, displayed a decreasing and an increasing tendency after the UV (365 nm, 3 W) irradiation, indicating that the *trans*-**Azo-16mer** has transformed into *cis*-**Azo-16mer** within 120 s. On the contrary, when exposed to visible light (450 nm, 3 W), the characteristic absorption bands were restored and indicated that the **Azo-16mer** underwent a change from the *cis* to the *trans* state. The absorption bands at 325 and 440 nm can be attributed to the typical $\pi-\pi^*$ and $n-\pi^*$ transitions of the azobenzene group of **Azo-16mer**, respectively.[27] Through alternating UV/vis light irradiation, this reversible photoisomerization process between *trans*-**Azo-16mer** and *cis*-**Azo-16mer** could be recycled more than 5 times (Figure S2). As expected, the self-assembled nanocapsules totally transformed into irregular aggregates after exposure to UV light (365 nm, 3 W) for 10 min, which could be clearly visualized by SEM and TEM images (Figure 2d,e). It results from the decomplexation process of α-CD and light-induced *cis*-**Azo-16mer**. The self-assembled nanocapsules of **Azo-4mer** ⊂ α-CD and **Azo-8mer** ⊂ α-CD also exhibited the same light-switchable disassembly−reassembly performances (Figures S3 and S4). In addition, the DLS instrument was also utilized to characterize the dynamic disassembly process of nanocapsules by real-time monitoring analysis. The hydrodynamic diameters of the nanocapsules have gradually increased from 295.3 to 531.2 nm under continuous UV light irradiation (Figures 2f and S5). During this process, the

https://doi.org/10.1021/jacsau.5c00762
JACS Au 2025, 5, 4439−4448

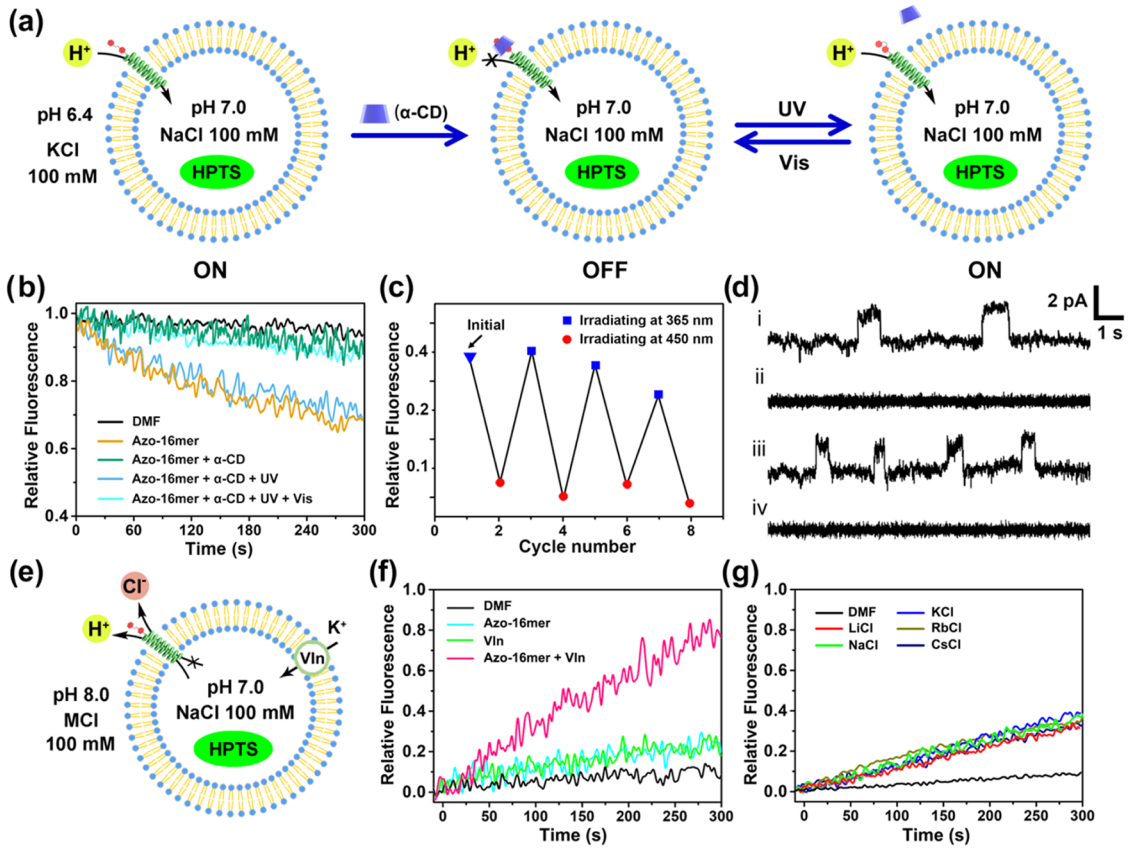

Figure 3. (a) Schematic representation of the light-sensitive proton transport behaviors of the supra-amphiphilic helix in EYPC-based LUVs. (b) HPTS assay of **Azo-16mer**, **Azo-16mer** ⊂ α-CD, and **Azo-16mer** ⊂ α-CD under UV and visible light irradiations, respectively. (c) Reversible variation of the normalized ion transport activities of **Azo-16mer** ⊂ α-CD according to the HPTS assay. (d) The patch clamp experiments of i: **Azo-16mer**, ii: **Azo-16mer** ⊂ α-CD, iii: ii + UV light irradiation, iv: iii + vis light irradiation in the symmetric baths (*cis* chamber = *trans* chamber = HCl, pH = 1) under an applied voltage of +150 mV; note: the molar ratio of **Azo-16mer** relative to phospholipids is about 2.81%. (e, f) The HPTS assay for assessing the proton transport activities of **Azo-16mer** in the presence or absence of valinomycin with intravesicular NaCl (pH = 7.0, 100 mM) and extravesicular MCl (M = K, pH = 8.0, 100 mM) solutions. (g) HPTS assay for assessing cation transport activities of **Azo-16mer** with intravesicular NaCl (pH = 7.0, 100 mM) and extravesicular MCl (M = Li, Na, K, Rb, Cs, pH = 8.0, 100 mM).

supramolecular structures of the helix-based nanocapsules were destroyed and transformed into irregular aggregates with a much larger size.

Ion Transport Activity and Selectivity

According to our previous report, the quinoline-derived **16mer** (without the azobenzene moiety) could selectively transport protons across the membranes at the single-molecule level owing to its small NH-rich luminal cavity.[28] Therefore, it is predictable that the guest molecule **Azo-16mer** may also act as a potential artificial proton channel due to its structural similarity with **16mer**. In consideration of the light sensitivity of **Azo-16mer** ⊂ α-CD, we wondered whether we could control the reversible ON/OFF proton transport activities by alternating UV/vis light irradiation on this ion transport system? It is predictable that the guest molecule **Azo-16mer** can insert into the hydrophobic region of lipid bilayers and serve as a unimolecular artificial channel to flux protons across the membranes. The introduction of hydrophilic α-CD will complex with **Azo-16mer** and then form a supra-amphiphilic helix **Azo-16mer** ⊂ α-CD, which will further hinder or even turn off the proton transport process. Under UV light irradiation, the hydrophobic *cis*-**Azo-16mer** will decomplex from α-CD, insert into the bilayer membranes, and restart the proton flux process, which can be closed by the irradiation of visible light (Figure 3a).

To verify our hypothesis, the pH-sensitive 8-hydroxypyrene-1,3,6-trisulfonic acid trisodium salt (HPTS) assay was first applied to estimate the proton transport activity of **Azo-16mer** via large unilamellar vesicles (LUVs), buffered by HEPES with intravesicular NaCl (pH = 7.0, 100 mM) and extravesicular KCl (pH = 6.4, 100 mM) solutions, respectively (Figure 3a). The LUVs were comprised of egg yolk L-a-phosphatidylcholine (EYPC) entrapping HPTS (1 mM) dye. The pH gradient across the bilayer membranes allows the transmembrane permeation of H^+ into the LUVs after injecting an artificial proton channel, which was subsequently evaluated by continuously monitoring the fluorescence intensity variation of the entrapped HPTS dye. As shown in Figure 3b, after injection of **Azo-16mer** (1.2 μM with a molar ratio to phospholipids of 0.51%) into the test solution, a significant fluorescence intensity decrease of ∼32% could be observed, suggesting that the extravesicular H^+ has been fluxed into the HPTS-trapped LUVs. While the addition of equimolar α-CD could significantly inhibit the proton transport activities of **Azo-16mer** because the supra-amphiphilic **Azo-16mer** ⊂ α-CD blocked the transmembrane nanopore of **Azo-16mer** due to the host−guest complexation between α-CD and the azobenzene groups on **Azo-16mer**. Interestingly, under the UV

https://doi.org/10.1021/jacsau.5c00762
JACS Au 2025, 5, 4439−4448

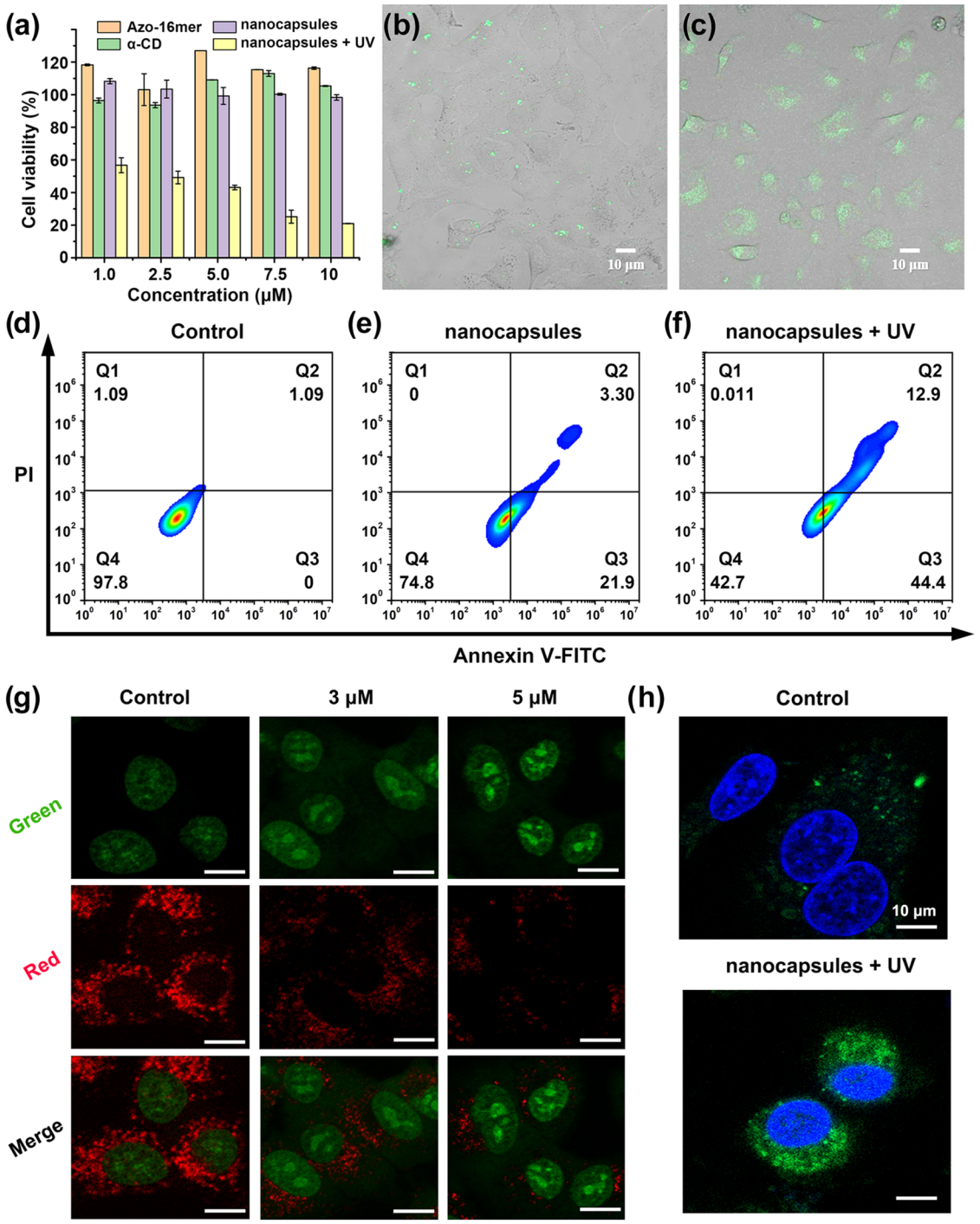

Figure 4. (a) Dose-dependent cell viability of A549 cells incubated with **Azo-16mer**, α-CD, and nanocapsules with and without UV light irradiation for 24 h according to the CCK-8 assay. (b) Representative CLSM images of the A549 cells incubated with the 5(6)-CF-loaded helix-based supramolecular nanocapsules for 12 h and then (c) exposed to UV light (365 nm, 3 W) irradiation for 10 min. Evaluation of A549 cell apoptosis by flow cytometry via treating with (d) DMF solution, (e) nanocapsules (10 μM), and (f) nanocapsules (10 μM) with UV light irradiation. FITC = fluorescein isothiocyanate. PI = propidium iodide. (g) Cell imaging of A549 cells treated with the post-UV-irradiated nanocapsules at the concentrations of 3 μM and 5 μM. Scale bar: 20 μm. This is followed by staining with AO dye. (h) Immunostaining of released cytochrome c in A549 cells upon the treatment of post-UV-irradiated NPCs (10 μM) for 12 h. Cytochrome c was stained with cytochrome c primary antibody (green), and 4′,6-diamidino-2-phenylindole (DAPI, blue) was used to mark the cell nuclei.

light (365 nm, 3 W) irradiation for 10 min, the **Azo-16mer** ⊂ α-CD will decomplex into water-soluble α-CD (outside the membrane) and *cis*-**Azo-16mer** (inside the membrane) with the recovered proton transport abilities. Besides, we also tested the proton transport capabilities of both *trans*- and *cis*-**Azo-16mer**, showing similar proton transport tendency (Figure S2d). By contrast, the visible light (450 nm, 3 W) irradiation further turned off this proton transport behavior along with the complexation of **Azo-16mer** ⊂ α-CD. Further investigation indicated that the reversible ON/OFF proton transport performances could be recycled more than four times and then gradually exhibited a fatigue effect according to the HPTS

https://doi.org/10.1021/jacsau.5c00762
JACS Au 2025, 5, 4439−4448

assay (Figure 3c). In contrast, the lengths of **Azo-4mer** and **Azo-8mer** are insufficient to span across the hydrophobic region of bilayer membranes (3.50 nm)[29] and therefore revealed a negligible transmembrane proton transport activity (Figure S6).

The reversible light-gated proton transport performance of **Azo-16mer** ⊂ α-CD was further estimated by patch clamping experiments on planar lipid bilayers in symmetric baths. As shown in Figure 3d, square-like conductance signals were detected after the addition of a small amount of **Azo-16mer** into the *cis* chamber (HCl, 0.1 M, pH = 1), indicating that the proton permeation resulted from a pore-containing channel rather than an ion carrier mechanism. Similar to the HPTS assay, the addition of equimolar α-CD can turn off the proton transport with similar ON/OFF switchable transport activities by alternate irradiation with UV and visible lights. Moreover, the ion selectivity was further estimated by the HPTS assay via loading NaCl (100 mM, pH = 7.0) and MCl (M = Li, Na, K, Rb, and Cs, 100 mM, pH = 8.0) buffer solutions inside and outside the vesicular membranes. As shown in Figure 3g, the **Azo-16mer** has triggered a similar H^+ efflux tendency with different extravesicular cations, indicating its inability to flux other alkali metal ions. It is noteworthy that valinomycin (Vln, a natural K^+-selective carrier) has significantly enhanced the proton transport degree (up to 80%) of **Azo-16mer** through balancing the membrane potential by the antiport of K^+ into LUVs. The extravesicular KCl buffer is necessary for balancing the membrane potential through the antiport H^+/K^+ exchange by Vln. As a control, pure Vln only caused a weak increase in the fluorescence intensity under the same conditions (Figure 3e,f). These results confirmed the H^+-selective transmembrane transport performance of **Azo-16mer** and its light-controlled ON/OFF transport behaviors with the assistance of α-CD complexation.

In Vitro Cancer Cell Apoptosis Induction

As is known, the prerequisite for the passive proton transport of the artificial H^+ channel lies in the different proton concentrations across the bilayer membranes. In the physiological environment, an obvious pH gradient exists mainly across the lysosomal membranes (pH_{inside} = 4.5−5.0) rather than other organelles or plasma membranes.[30] In consideration of the light-sensitive proton transport and self-assembled behaviors of supra-amphiphilic helix **Azo-16mer** ⊂ α-CD, we wondered whether it is possible to deliver the nanocapsules into cancer cells and then release **Azo-16mer** under UV light irradiation, which could further insert into lysosomal membranes and trigger cell apoptosis.[22] Therefore, the cytotoxicity of **Azo-16mer**, α-CD, nanocapsules, and nanocapsules under UV light irradiation against A549 (human lung adenocarcinoma cell line) was evaluated by employing the CCK-8 (Cell Counting Kit-8) assay. As shown in Figure 4a, **Azo-16mer**, α-CD, and nanocapsules showed nontoxicity toward the A549 (human nonsmall cell lung cancer cells) under the given concentrations, while the nanocapsules with UV light irradiation manifested considerable toxicity with an IC50 (half-maximum inhibitory concentration) value of 5.8 μM (Figure S7). Similar cytotoxicity was also observed when the supramolecular nanocapsules were incubated with B16 and 4T1 cells (Figures S8 and S9). Understandably, **Azo-16mer** can insert into only the cell membrane of A549, wherein the proton gradient is negligible and insufficient to disrupt the ion homeostasis of cancer cells. By contrast, the nanocapsules composed of **Azo-16mer** ⊂ α-CD can be taken up and release **Azo-16mer** in the cytosol of cancer cells, which further neutralize the acidic environments of lysosomes via flux protons out of their membrane.[19] Undoubtedly, no cytotoxicity was detected for the self-assembled nanocapsules of **Azo-4mer** ⊂ α-CD and **Azo-8mer** ⊂ α-CD (Figure S10). The endocytosis process and light-triggered release performance of nanocapsules were further characterized by confocal laser scanning microscopy (CLSM). The 5(6)-carboxy fluorescein (5(6)-CF, a commonly used fluorescent dye), was loaded into the nanocapsules for fluorescence tracing, and green dots were clearly visualized after coincubation with A549 cells for 4 h (Figure 4b). After UV light (365 nm, 3 W) irradiation for 10 min, green fluorescent dye filled the cytoplasm of cancer cells, indicating that the nanocapsules turned to disassembly and release 5(6)-CF dye inside tumors under the UV light (Figure 4c).

To confirm the cell death mechanism, an apoptosis assay using fluorescein-conjugated Annexin V and propidium iodide (PI) staining was performed by flow cytometry. As depicted in Figure 4e, when incubated with nanocapsules at a concentration of 10 μM, the A549 cells yielded early and late apoptotic cell ratios of 21.9% and 3.3%, respectively, indicating relatively weak apoptosis-inducing capability. When irradiated for 10 min by UV (10 W) light, the early and late apoptotic cell ratios significantly increased to 44.4% and 12.9% (Figure 4f), strikingly contrasting with the low apoptotic ratios of control groups (0% early, 1.09% late; Figure 4d). Additionally, the side effects of UV light irradiation on cancer cells were ruled out by the same CCK-8 and flow cytometry experiments (Figure S11). These results indicated that the light-triggered disassembly of nanocapsules and release of **Azo-16mer** played pivotal roles in the cell apoptotic process. As mentioned before, **Azo-16mer** is an artificial proton channel that may cause proton efflux from acidic organelles (such as lysosomes) inside tumor cells. Therefore, the impact of light-sensitive nanocapsules on lysosomal pH was evaluated by acridine orange (AO) staining assay. The pH-sensitive AO emits orange fluorescence in acidic compartments of lysosomes and green fluorescence when the pH value is elevated.[31] As shown in Figure 4g, after incubating the A549 cells with nanocapsules (c = 3 μM, 5 μM) and of AO (50 μM), the UV light irradiation triggered a concentration-dependent intensity decrease in red fluorescence and an increase in green fluorescence, indicating a decrease of acidity and pH increase in lysosomes. Next, SNARF-1 (a pH-sensitive dye) was applied to evaluate the acidification of cytosol. Due to the effective disruption of proton gradients by proton channels, the A549 cells treated with nanocapsules with UV light irradiation showed enhanced green fluorescence compared to the control group, indicating the process of cytoplasmic acidification (Figure S14).

As is known, one of the hallmark features of apoptosis is the loss of mitochondrial membrane potential (MMP) and we therefore employed the JC-1 probe to conduct MMP characterization, which formed J-aggregates and revealed red fluorescence in healthy mitochondria and green fluorescence in depolarized mitochondria.[32] After treatment of A549 cells with nanocapsules at concentrations of 5 and 10 μM, UV light irradiation, and incubation with the JC-1 probe, we can observe a concentration-dependent decrease in red fluorescence along with an enhancement of green fluorescence, and the variation of MMP was quantified by calculating the pixel intensity ratio (I_{red} /I_{green}), revealing $a \approx$ 94.0% decrease in the

https://doi.org/10.1021/jacsau.5c00762
JACS Au 2025, 5, 4439−4448

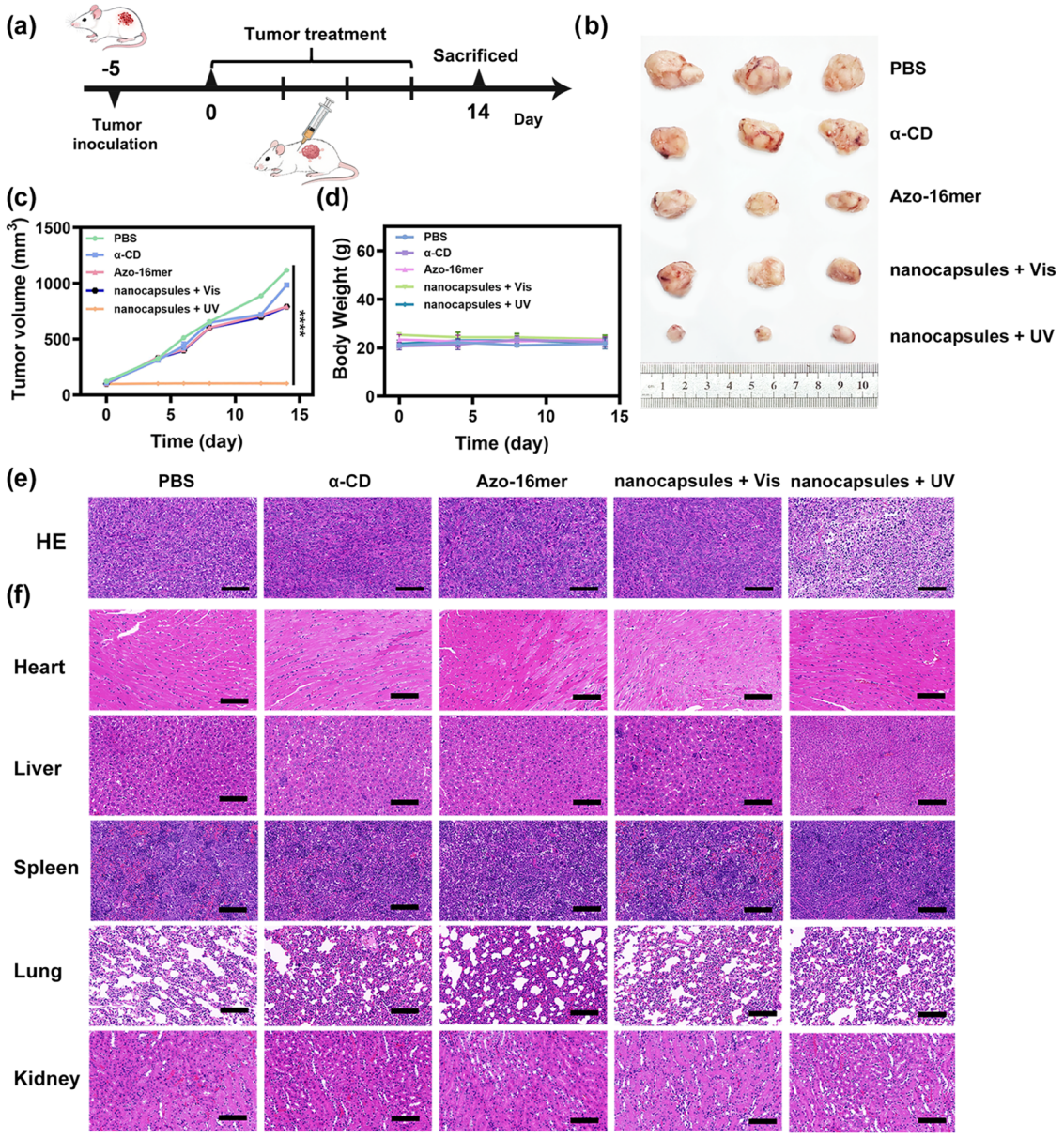

Figure 5. In vivo antitumor efficacy evaluation of the nanocapsules. (a) Schematic diagram of the establishment of a mouse breast 4T1 cancer model. (b) Photograph of tumors removed from mice from different treatment groups. (c) Curves of the tumor volume changes of different groups in the treatment periods (mean ± SD, $n = 3$; the statistical significance was acquired by one-way ANOVA, ****$p < 0.0001$). (d) Curves of body weight in different treatment groups over time. (e) H&E staining for pathological changes in tumor tissues collected from different groups; scale bar: 100 μm. (f) Histopathological examinations of major organs from mice with different treatments by H&E staining; scale bar: 100 μm.

post-UV-treated nanocapsule group, demonstrating an unambiguous depolarization of MMP (Figure S12). Besides the loss of MMP, the impairment of lysosomal functions is closely related to the disruption of the autophagy process, which also plays essential roles in living organisms to maintain cellular homeostasis.[11,19] As is known, the MMP depolarization is closely related to the upregulation of harmful reactive oxygen species (ROS), as confirmed by using the 2′,7′-dichlorodihydrofluorescein diacetate (DCFH-DA) probe.[33,34] After incubating A549 cells with nanocapsules and DCFH-DA, the UV light irradiation triggered a gradual increase of the green fluorescence intensity accompanied by the increased concentration of PNCs (Figure S13). In the apoptotic pathway, the high concentration of the intracellular ROS level can trigger the opening of mitochondrial permeability transition pores (PTPs), promoting the release of cytochrome c from the mitochondria into the cytoplasm.[34] Therefore, immunofluorescence staining by cytochrome c primary antibody was performed to estimate the concentration variations of cytochrome c in the cytoplasm. As shown in Figure 4h, the A549 cell-incubated nanocapsules (10 μM) showed significantly enhanced green fluorescence compared with the control group after being treated with UV light irradiation, implying that cytochrome c has leaked from mitochondria to the cytoplasm owing to the activation of mitochondrial PTPs.

In Vivo Antitumor Activity

To further investigate the tumor-inhibiting efficacy of nanocapsules in vivo, the subcutaneous 4T1 BALB/c mouse model was employed according to the treatment protocol in Figure 5a. When the tumors reached the size of ≈100 mm^3, the mice

https://doi.org/10.1021/jacsau.5c00762
JACS Au 2025, 5, 4439−4448

with tumors were randomly divided into five groups and treated with the intratumoral injection of PBS, α-CD, **Azo-16mer**, nanocapsules, and nanocapsules with UV light. The therapeutic effects of these groups were routinely monitored over a 14 day period. No tumor growth impairment was observed in mice treated with α-CD, **Azo-16mer**, and nanocapsules, which is consistent with the previous in vitro toxicity assessments. Notably, a substantial reduction in tumor development was observed in the nanocapsule group following UV light irradiation (10 W, 15 min) compared to control groups, confirming its superior antitumor performance, with a tumor inhibition rate as high as 92.49% (Figure 5b,c). This can be attributed to the UV-induced disassembly of helix-based nanocapsules, triggering the release of **Azo-16mer** for mediating proton transport across lysosomal membranes. The directional efflux of H^+ from the lysosomal lumen to the cytosol induced lysosomal alkalization, which further initiated a cascade of molecular events that culminated in cancer cell apoptosis. Meanwhile, the toxicity assay results of 4T1 cells subjected to a 15 min UV light irradiation showed no significant damage, ruling out the impact of UV light on the cells. Additionally, we also examined the body weight of mice during the treatment to test the biocompatibility of the nanocapsules. As shown in Figure 5d, all animal groups showed negligible body weight changes, indicating that these helical-based nanocapsules are safe and reliable.

Furthermore, the H&E staining images of the main organs, including the heart, liver, spleen, lung, and kidney, showed a normal, defect-free, organizational structure without hemorrhage and inflammatory infiltration, indicating that the nanocapsules did not cause substantial harm to major organs (Figure 5f). Both the in vitro and in vivo experiments have demonstrated that the artificial proton channel-based nanocapsules have shown desirable biosafety and antitumor efficacy, which can transfer proton channels into cancer cells and induce apoptosis by disrupting the intracellular ion homeostasis of tumor cells.

CONCLUSIONS

In summary, we have presented here a de novo-designed ion channel delivery system (ICDS) based on the light-sensitive nanocapsule self-assembled host−guest complex of **Azo-16mer** ⊂ α-CD. Interestingly, the nanocapsules can easily enter cancer cells by endocytosis and release the artificial proton channels upon UV light irradiation, which revealed a desirable anticancer effect through interfering with the ion homeostasis and elevating the pH level of acidic lysosomes inside tumor cells. Subsequently, the loss of mitochondrial membrane potential, release of cytochrome c from mitochondria, and increase in the reactive oxygen species level in the cytosol have jointly validated the apoptotic cell death mechanism. Both in vitro and in vivo experiments have confirmed the anticancer efficacy and biosafety of this artificial helix-based light-sensitive ICDS. Importantly, this work has established an ion-interference antitumor strategy through the ion channel delivery system by incorporating artificial ion channels inside the delivery platform. It is anticipated that this work will not only provide beneficial inspiration for fabricating novel drug delivery platforms but also contribute to exploring future therapeutic directions for artificial ion channels.

ASSOCIATED CONTENT

Supporting Information

The Supporting Information is available free of charge at https://pubs.acs.org/doi/10.1021/jacsau.5c00762.

Details regarding the synthesis of **Azo-16mer**, **Azo-8mer**, and **Azo-4mer** (Scheme S1); schematic representation of the supra-amphiphilic helix (Figure S1); UV−vis spectroscopic characterization (Figure S2); morphological characterization (Figures S3−S5); ion transport assays of **Azo-8mer** and **Azo-4mer** (Figure S6); biological studies (Figures S7−S14); and spectrum of **Azo-8mer** and **Azo-16mer** and MALDI-TOF MS of **Azo-8mer** and **Azo-16mer** (Figures S15−S18) (PDF)

AUTHOR INFORMATION

Corresponding Authors

Tengfei Yan − *Key Laboratory of Organosilicon Chemistry and Material Technology, Ministry of Education, Zhejiang Key Laboratory ofOrganosilicon Material Technology, College of Material, Chemistry and Chemical Engineering, Hangzhou Normal University, Hangzhou 311121 Zhejiang, China*; Email: tengfeiyan@163.com

Junqiu Liu − *Key Laboratory of Organosilicon Chemistry and Material Technology, Ministry of Education, Zhejiang Key Laboratory ofOrganosilicon Material Technology, College of Material, Chemistry and Chemical Engineering, Hangzhou Normal University, Hangzhou 311121 Zhejiang, China*; orcid.org/0000-0003-1608-7908; Email: junqiuliu@jlu.edu.cn

Authors

Yueyue Lu − *Key Laboratory of Organosilicon Chemistry and Material Technology, Ministry of Education, Zhejiang Key Laboratory ofOrganosilicon Material Technology, College of Material, Chemistry and Chemical Engineering, Hangzhou Normal University, Hangzhou 311121 Zhejiang, China*

Yuxin Wu − *Key Laboratory of Organosilicon Chemistry and Material Technology, Ministry of Education, Zhejiang Key Laboratory ofOrganosilicon Material Technology, College of Material, Chemistry and Chemical Engineering, Hangzhou Normal University, Hangzhou 311121 Zhejiang, China*

Canhong Zhu − *Key Laboratory of Organosilicon Chemistry and Material Technology, Ministry of Education, Zhejiang Key Laboratory ofOrganosilicon Material Technology, College of Material, Chemistry and Chemical Engineering, Hangzhou Normal University, Hangzhou 311121 Zhejiang, China*

Tianlong Zhang − *Key Laboratory of Organosilicon Chemistry and Material Technology, Ministry of Education, Zhejiang Key Laboratory ofOrganosilicon Material Technology, College of Material, Chemistry and Chemical Engineering, Hangzhou Normal University, Hangzhou 311121 Zhejiang, China*

Yanting Wu − *Key Laboratory of Organosilicon Chemistry and Material Technology, Ministry of Education, Zhejiang Key Laboratory ofOrganosilicon Material Technology, College of Material, Chemistry and Chemical Engineering, Hangzhou Normal University, Hangzhou 311121 Zhejiang, China*

Lulu Xi − *Key Laboratory of Organosilicon Chemistry and Material Technology, Ministry of Education, Zhejiang Key*

https://doi.org/10.1021/jacsau.5c00762
JACS Au 2025, 5, 4439−4448

Laboratory ofOrganosilicon Material Technology, College of Material, Chemistry and Chemical Engineering, Hangzhou Normal University, Hangzhou 311121 Zhejiang, China

Xianze Huang − *Key Laboratory of Organosilicon Chemistry and Material Technology, Ministry of Education, Zhejiang Key Laboratory ofOrganosilicon Material Technology, College of Material, Chemistry and Chemical Engineering, Hangzhou Normal University, Hangzhou 311121 Zhejiang, China*

Complete contact information is available at: https://pubs.acs.org/10.1021/jacsau.5c00762

Notes

The authors declare no competing financial interest.

■ ACKNOWLEDGMENTS

This work was supported by the National Natural Science Foundation of China (No. 22275046), the Hangzhou Leading Innovation and Entrepreneurship Team Project (TD2022001), and the Interdisciplinary Research Project of Hangzhou Normal University (2024JCXK01).

■ REFERENCES

(1) Hille, B. Ionic Channels of Excitable Membranes, Sinauer Assoc. Inc., Sunderland, MA, 2001.
(2) Zaydman, M. A.; Silva, J. R.; Cui, J. Ion Channel Associated Diseases: Overview of Molecular Mechanisms. *Chem. Rev.* **2012**, *112* (12), 6319−6333.
(3) Lin, J.-F.; Wang, X.-D.; Ao, Y.-F.; Wang, Q.-Q.; Wang, D.-X. Spontaneous Transition between Multiple Conductance States and Rectifying Behaviors in an Artificial Single-Molecule Funnel. *Angew. Chem., Int. Ed.* **2024**, *63* (40), No. e202411702.
(4) Huang, W.-L.; Wang, X.-D.; Ao, Y.-F.; Wang, Q.-Q.; Wang, D.-X. Artificial Chloride-Selective Channel: Shape and Function Mimic of the ClC Channel Selective Pore. *J. Am. Chem. Soc.* **2020**, *142* (31), 13273−13277.
(5) Cao, R.; Rossdeutcher, R. B.; Zhong, Y.; Shen, Y.; Miller, D. P.; Sobiech, T. A.; Wu, X.; Buitrago, L. S.; Ramcharan, K.; Gutay, M. I.; et al. Aromatic pentaamide macrocycles bind anions with high affinity for transport across biomembranes. *Nat. Chem.* **2023**, *15* (11), 1559−1568.
(6) Muraglia, K. A.; Chorghade, R. S.; Kim, B. R.; Tang, X. X.; Shah, V. S.; Grillo, A. S.; Daniels, P. N.; Cioffi, A. G.; Karp, P. H.; Zhu, L.; et al. Small-molecule ion channels increase host defences in cystic fibrosis airway epithelia. *Nature* **2019**, *567* (7748), 405−408.
(7) Yang, L.; Han, B.; Zhang, M.; Wang, Y.-H.; Tao, K.; Zhu, M. X.; He, K.; Zhang, Z.-G.; Hou, S. Activation of BK Channels Prevents Hepatic Stellate Cell Activation and Liver Fibrosis Through the Suppression of TGFβ1/SMAD3 and JAK/STAT3 Profibrotic Signaling Pathways. *Front. Pharmacol.* **2020**, *11*, No. 165.
(8) Zhang, Q.; Liang, Q.; Wang, G.; Xie, X.; Cao, Y.; Sheng, N.; Zeng, Z.; Ren, C. Highly Selective Artificial K^+ Transporters Reverse Liver Fibrosis In Vivo. *JACS Au* **2024**, *4* (10), 3869−3883.
(9) Yan, T.; Zheng, X.; Liu, S.; Zou, Y.; Liu, J. Ion transporters: emerging agents for anticancer therapy. *Sci. China Chem.* **2022**, *65* (7), 1265−1278.
(10) Saha, T.; Gautam, A.; Mukherjee, A.; Lahiri, M.; Talukdar, P. Chloride Transport through Supramolecular Barrel-Rosette Ion Channels: Lipophilic Control and Apoptosis-Inducing Activity. *J. Am. Chem. Soc.* **2016**, *138* (50), 16443−16451.
(11) Mondal, A.; Save, S. N.; Sarkar, S.; Mondal, D.; Mondal, J.; Sharma, S.; Talukdar, P. A Benzohydrazide-Based Artificial Ion Channel that Modulates Chloride Ion Concentration in Cancer Cells and Induces Apoptosis by Disruption of Autophagy. *J. Am. Chem. Soc.* **2023**, *145* (17), 9737−9745.
(12) Malla, J. A.; Umesh, R. M.; Yousf, S.; Mane, S.; Sharma, S.; Lahiri, M.; Talukdar, P. A Glutathione Activatable Ion Channel Induces Apoptosis in Cancer Cells by Depleting Intracellular Glutathione Levels. *Angew. Chem., Int. Ed.* **2020**, *59* (20), 7944−7952.
(13) Jia, C.; Luo, D.; Zhou, J.; Xie, X.; Yuen In Lam, H.; Li, P.; Mu, Y.; Zeng, Z.; Ren, C. Engineered Reactive Oxygen Species (ROS)-Responsive Artificial H^+/Cl^- Ion Channels for Targeted Cancer Treatment. *Angew. Chem., Int. Ed.* **2024**, *64*, No. e202419800.
(14) Zhang, M.; Song, R.; Liu, Y.; Yi, Z.; Meng, X.; Zhang, J.; Tang, Z.; Yao, Z.; Liu, Y.; Liu, X.; Bu, W. Calcium-Overload-Mediated Tumor Therapy by Calcium Peroxide Nanoparticles. *Chem* **2019**, *5* (8), 2171−2182.
(15) Liu, Y.; Zhang, M.; Bu, W. Bioactive nanomaterials for ion-interference therapy. *View* **2020**, *1* (2), No. e18.
(16) Wu, Y.; Li, C.; Wu, Y.; Xu, J.; Ni, Z.; Reany, O.; Yan, T.; Zhu, D.; Liu, J. A Reversible Light-Driven Biomimetic K^+/Na^+-Exchanger Controls Cancer Cell Apoptosis. *Adv. Funct. Mater.* **2024**, *34* (29), No. 2400432.
(17) Lee, D.; Lee, S.-H.; Noh, I.; Oh, E.; Ryu, H.; Ha, J.; Jeong, S.; Yoo, J.; Jeon, T.-J.; Yun, C.-O.; Kim, Y. A Helical Polypeptide-Based Potassium Ionophore Induces Endoplasmic Reticulum Stress-Mediated Apoptosis by Perturbing Ion Homeostasis. *Adv. Sci.* **2019**, *6* (14), No. 1801995.
(18) Busschaert, N.; Park, S.-H.; Baek, K.-H.; Choi, Y. P.; Park, J.; Howe, E. N. W.; Hiscock, J. R.; Karagiannidis, L. E.; Marques, I.; Félix, V.; et al. A synthetic ion transporter that disrupts autophagy and induces apoptosis by perturbing cellular chloride concentrations. *Nat. Chem.* **2017**, *9* (7), 667−675.
(19) Zhong, Q.; Cao, Y.; Xie, X.; Wu, Y.; Chen, Z.; Zhang, Q.; Jia, C.; Wu, Z.; Xin, P.; Yan, X.; et al. Non-Covalently Stapled H^+/Cl^- Ion Channels Activatable by Visible Light for Targeted Anticancer Therapy. *Angew. Chem., Int. Ed.* **2024**, *63* (3), No. e202314666.
(20) Xu, H.; Martinoia, E.; Szabo, I. Organellar channels and transporters. *Cell Calcium* **2015**, *58* (1), 1−10.
(21) Matamala, E.; Castillo, C.; Vivar, J. P.; Rojas, P. A.; Brauchi, S. E. Imaging the electrical activity of organelles in living cells. *Commun. Biol.* **2021**, *4* (1), No. 389.
(22) Shen, F.-F.; Dai, S.-Y.; Wong, N.-K.; Deng, S.; Wong, A. S.-T.; Yang, D. Mediating K^+/H^+ Transport on Organelle Membranes to Selectively Eradicate Cancer Stem Cells with a Small Molecule. *J. Am. Chem. Soc.* **2020**, *142* (24), 10769−10779.
(23) Ryder, W. G.; Levina, A.; Graziotto, M. E.; Hawkins, B. A.; Hibbs, D. E.; New, E. J.; Gale, P. A. Subcellular targeted anion transporters. *Chem* **2025**, *11*, No. 102247.
(24) Manzari, M. T.; Shamay, Y.; Kiguchi, H.; Rosen, N.; Scaltriti, M.; Heller, D. A. Targeted drug delivery strategies for precision medicines. *Nat. Rev. Mater.* **2021**, *6* (4), 351−370.
(25) Gao, J.; Karp, J. M.; Langer, R.; Joshi, N. The Future of Drug Delivery. *Chem. Mater.* **2023**, *35* (2), 359−363.
(26) Yan, T.; Li, F.; Tian, J.; Wang, L.; Luo, Q.; Hou, C.; Dong, Z.; Xu, J.; Liu, J. Biomimetic Pulsating Vesicles with Both pH-Tunable Membrane Permeability and Light-Triggered Disassembly−Reassembly Behaviors Prepared by Supra-Amphiphilic Helices. *ACS Appl. Mater. Interfaces* **2019**, *11* (34), 30566−30574.
(27) Wang, Y.; Ma, N.; Wang, Z.; Zhang, X. Photocontrolled Reversible Supramolecular Assemblies of an Azobenzene-Containing Surfactant with α-Cyclodextrin. *Angew. Chem., Int. Ed.* **2007**, *46* (16), 2823−2826.
(28) Yan, T.; Liu, S.; Xu, J.; Sun, H.; Yu, S.; Liu, J. Unimolecular Helix-Based Transmembrane Nanochannel with a Smallest Luminal Cavity of 1 Å Expressing High Proton Selectivity and Transport Activity. *Nano Lett.* **2021**, *21* (24), 10462−10468.
(29) Gokel, G. W.; Mukhopadhyay, A. Synthetic models of cation-conducting channels. *Chem. Soc. Rev.* **2001**, *30* (5), 274−286.
(30) Gros, F.; Muller, S. The role of lysosomes in metabolic and autoimmune diseases. *Nat. Rev. Nephrol.* **2023**, *19* (6), 366−383.
(31) Wang, F.; Gómez-Sintes, R.; Boya, P. Lysosomal membrane permeabilization and cell death. *Traffic* **2018**, *19* (12), 918−931.

(32) Salvioli, S.; Ardizzoni, A.; Franceschi, C.; Cossarizza, A. JC-1, but not DiOC6(3) or rhodamine 123, is a reliable fluorescent probe to assess ΔΨ changes in intact cells: implications for studies on mitochondrial functionality during apoptosis. *FEBS Lett.* **1997**, *411* (1), 77−82.
(33) Sabharwal, S. S.; Schumacker, P. T. Mitochondrial ROS in cancer: initiators, amplifiers or an Achilles' heel? *Nat. Rev. Cancer* **2014**, *14* (11), 709−721.
(34) Chen, Z.; Xie, X.; Jia, C.; Zhong, Q.; Zhang, Q.; Luo, D.; Cao, Y.; Mu, Y.; Ren, C. Concentration-Driven Evolution of Adaptive Artificial Ion Channels or Nanopores with Specific Anticancer Activities. *Angew. Chem., Int. Ed.* **2024**, *63* (17), No. e202318811.

https://doi.org/10.1021/jacsau.5c00762
JACS Au 2025, 5, 4439−4448